

Supplementary Materials for

Plasmon-induced ultrafast charge transfer in single-particulate copper sulfide-zinc sulfide nanoheterostructures

Xueyi Guo,^{ac} Sheng Liu,^{ac} Weijia Wang,^{*bc} Chongyao Li,^{ac} Ying Yang,^{ac} Qinghua Tian,^{ac} and Yong Liu^{bc}

^a School of Metallurgy and Environment, Central South University, Changsha 410083, China

^b State Key Laboratory for Powder Metallurgy, Powder Metallurgy Research Institute, Central South University, Changsha 410083, China

^c Research Institute of Resource Recycling, Central South University, Changsha 410083, China

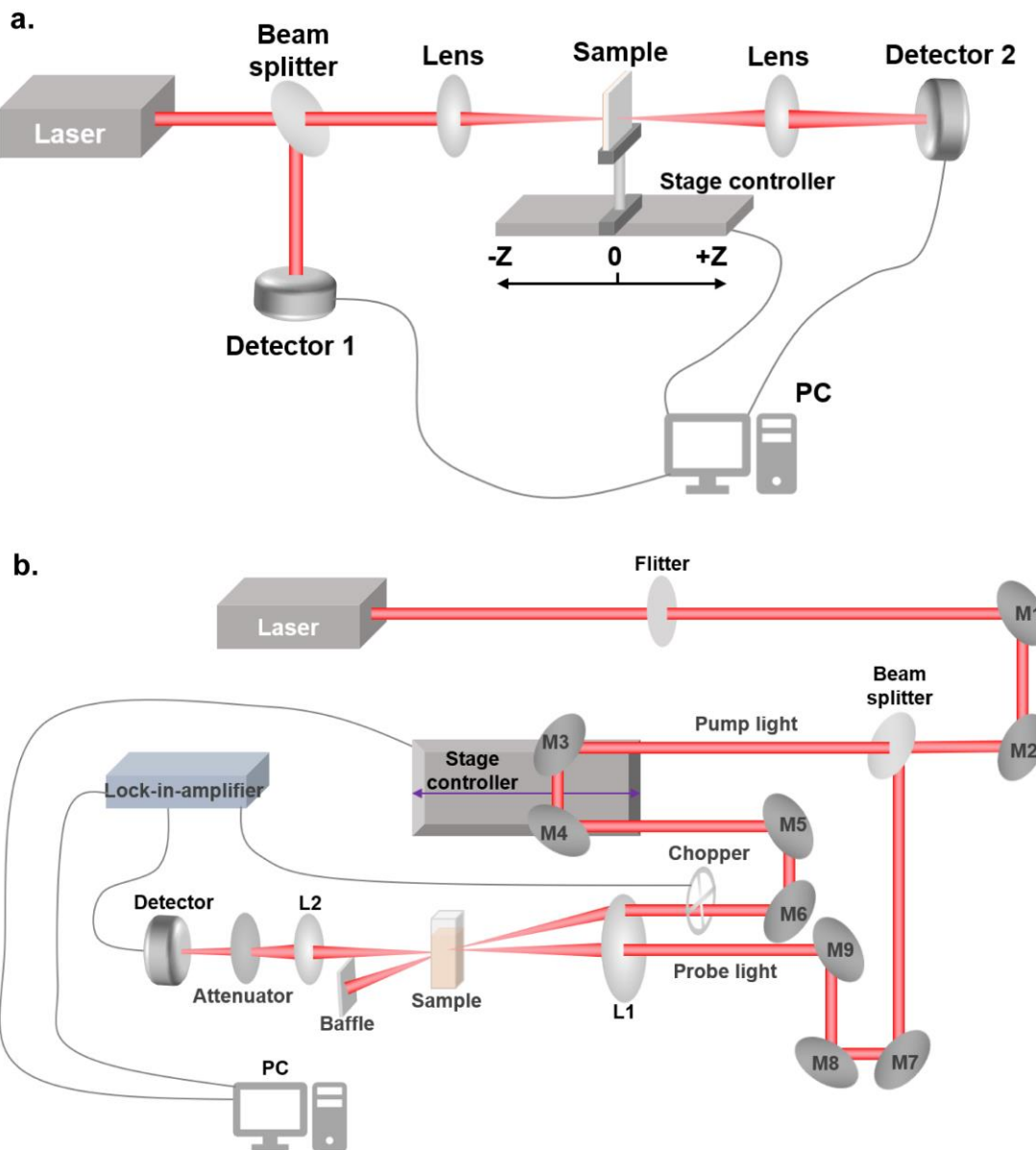
* Corresponding author at:

State Key Laboratory for Powder Metallurgy, Powder Metallurgy Research Institute, Central South University, Changsha 410083, China. E-mail address: wangweijia@csu.edu.cn (Weijia Wang).

This PDF file includes:

- **Scheme S1**
- **Fig. S1 to S8**
- **Table S1 to S3**
- **References**

- Supplementary Materials: Scheme S1.



Scheme S1. (a) Z-scan experimental setup. (b) Pump-Probe experimental setup: M1-M9: Mirrors; L1-L2: Lens.

- **Supplementary Materials: Fig. S1.**

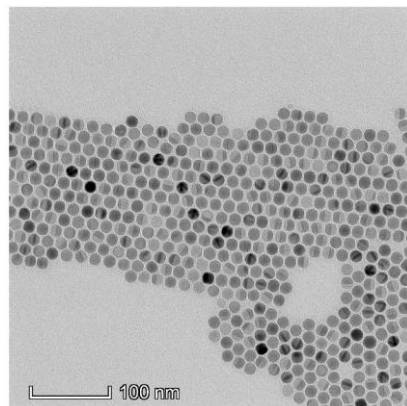


Fig. S1 Low magnification TEM images of $\text{Cu}_{1.94}\text{S}$ -ZnS NHs.

- **Supplementary Materials: Fig. S2.**

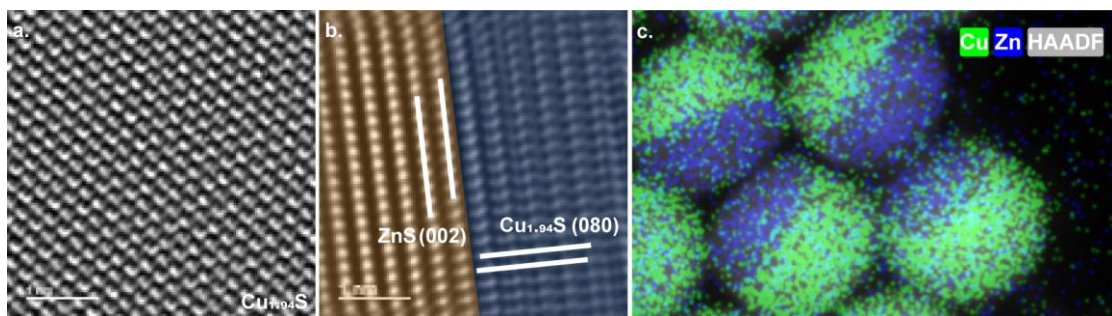


Fig. S2 Local enlarged HRTEM images of $\text{Cu}_{1.94}\text{S}$ NCs (a) and $\text{Cu}_{1.94}\text{S}$ -ZnS NHs (b) after a fast Fourier transform (FFT) process using DigitalMicrograph software. (c) Merged image of EDS element maps and HAADF-STEM.

- **Supplementary Materials: Fig. S3**

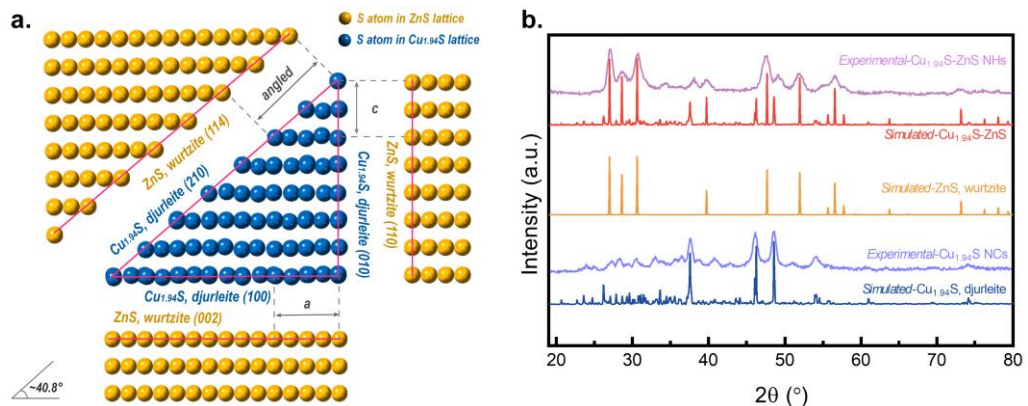


Fig. S3 (a) Idealized projections of the crystal planes of sulfur sublattice in wurtzite ZnS and djurleite $\text{Cu}_{1.94}\text{S}$. (b) Simulated XRD patterns of djurleite $\text{Cu}_{1.94}\text{S}$, wurtzite ZnS, and merged $\text{Cu}_{1.94}\text{S}$ (45%)-ZnS (55%). The crystallographic information files (CIFs) of standard djurleite $\text{Cu}_{1.94}\text{S}$ and wurtzite ZnS were acquired from the American **Supplementary Materials: Page S3**

Mineralogist Crystal Structure Database. **Djurleite Cu_{1.94}S:** Monoclinic, $a=26.8970\text{ \AA}$, $b=15.7450\text{ \AA}$, $c=13.5650\text{ \AA}$, $\beta=90.13^\circ$, P2_{1/n}.¹ **Wurtzite ZnS:** Hexagonal, $a=3.8110\text{ \AA}$, $c=6.2340\text{ \AA}$, P6_{3mc}.² The fractions of Cu_{1.94}S and ZnS in the merged simulated XRD pattern were referenced from the XPS results of the real sample with appreciated adjustment. The crystallographic projections were generated using CrystalMaker® software, and the simulated and merged XRD patterns were generated using CrystalDiffract® software.

- **Supplementary Materials: Fig. S4.**

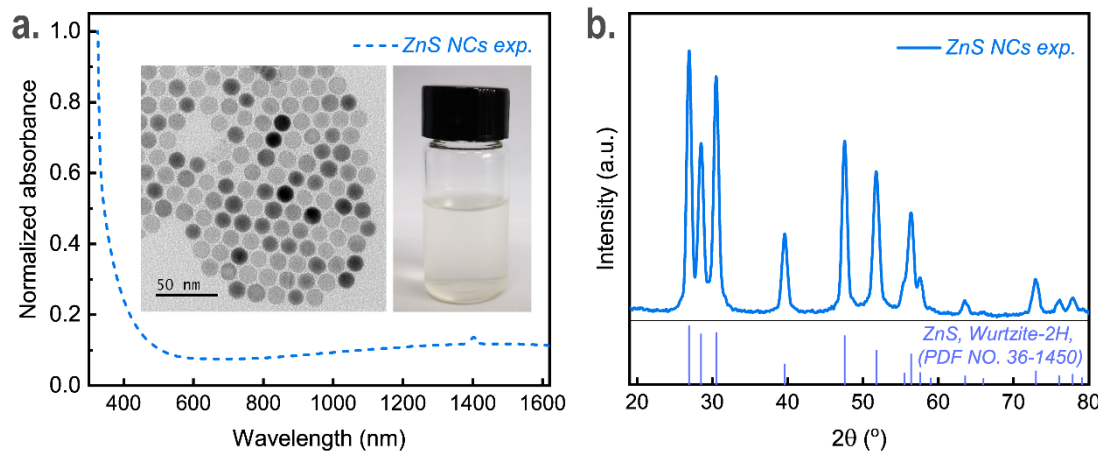


Fig. S4 Key characterization of ZnS NCs. (a) UV-vis-NIR absorption spectra and (b) XRD result. Inset: TEM image and digital photograph of ZnS NCs dispersed in NMP.

- **Supplementary Materials: Fig. S5.**

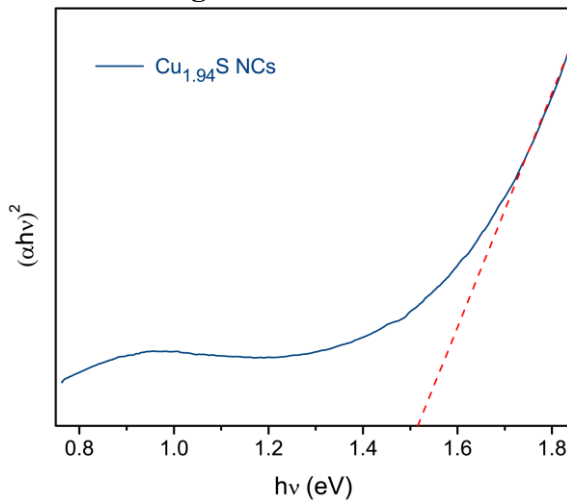


Fig. S5 $(\alpha h\nu)^2$ - $h\nu$ curve of the Cu_{1.94}S NCs

- **Supplementary Materials: Fig. S6.**

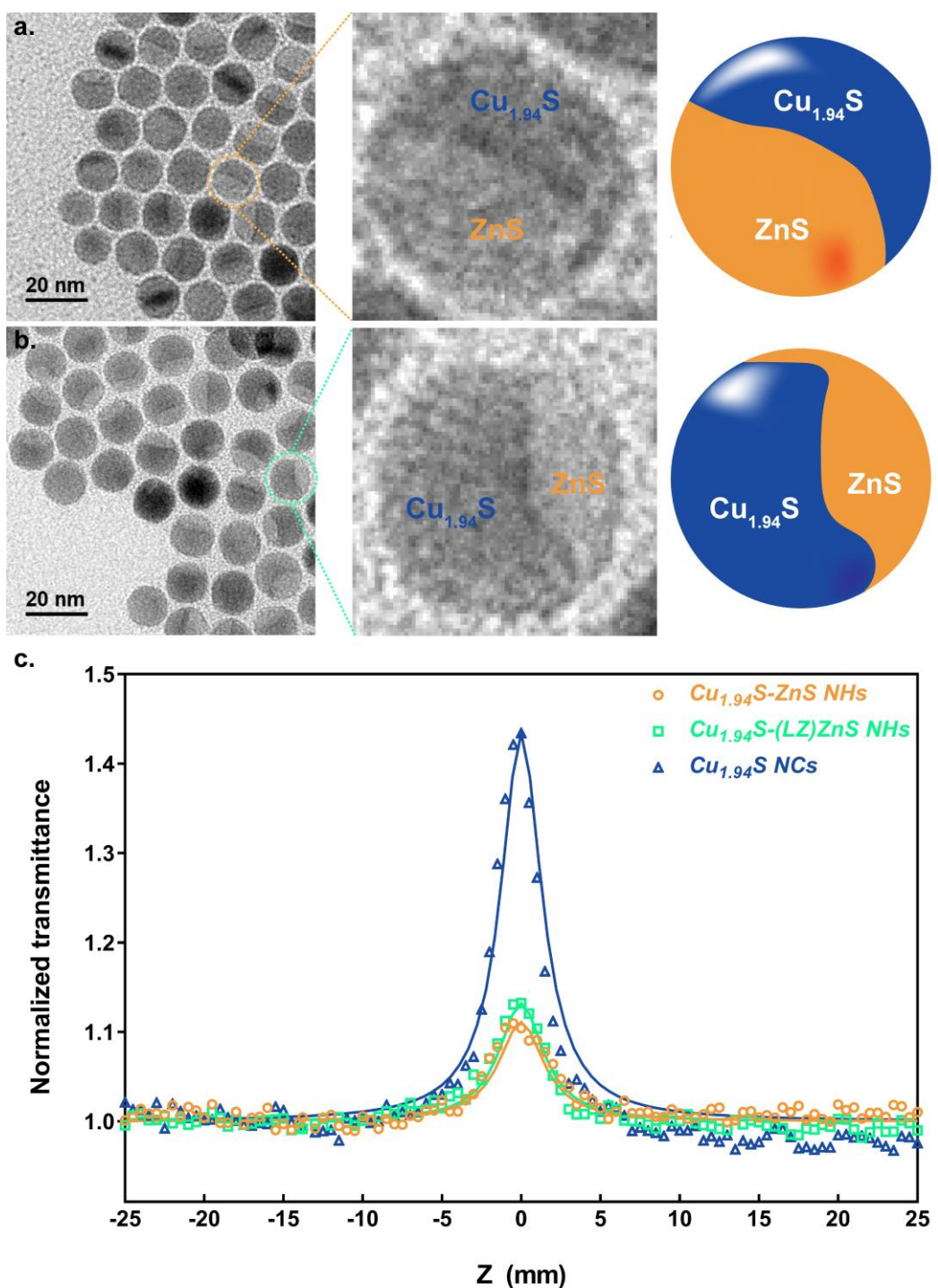


Fig. S6 TEM images of Cu_{1.94}S-ZnS NHs (a) and Cu_{1.94}S-(LZ)ZnS NHs (b). (c) Open-aperture Z-scan results of different samples at 1500 nm with identical input intensity.

- **Supplementary Materials: Fig. S7.**

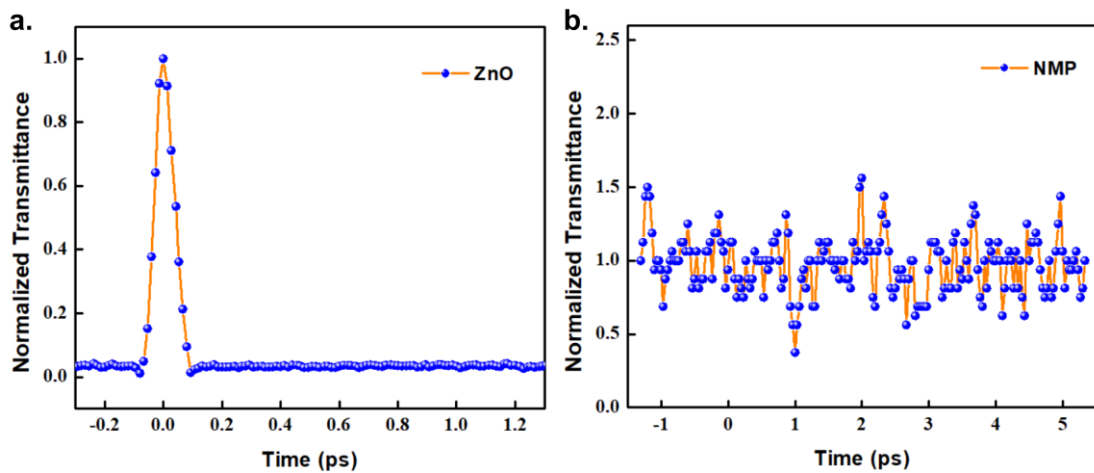


Fig. S7 Pump-probe results for the standard sample (a) and solvent (b).

- **Supplementary Materials: Fig. S8.**

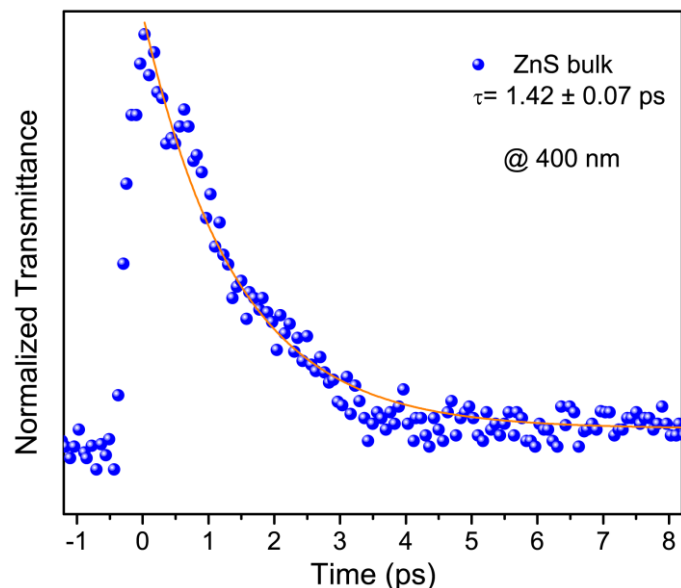


Fig. S8 Pump-probe signals of bulk ZnS.

- **Supplementary Materials: Table S1.**

Table S1. Lattice parameters of djurleite Cu_{1.94}S, roxbyite Cu_{1.8}S, and digenite Cu_{1.8}S

Lattice parameters	Cu _{1.94} S, <i>djurleite</i> ¹	Cu _{1.8} S, <i>roxbyite</i> ³	Cu _{1.8} S, <i>digenite</i> ⁴
<i>a</i> (Å)	26.8970	13.4090	5.5820
<i>b</i> (Å)	15.7450	13.4051	5.5820
<i>c</i> (Å)	13.5650	15.4852	5.5820
<i>α</i> (°)	90.000	90.022	90.000
<i>β</i> (°)	90.130	90.021	90.000
<i>γ</i> (°)	90.000	90.020	90.000
Spacegroup	P 2 _{1/n}	P T	F m 3m

- **Supplementary Materials: Table S2.**

Table S2. The lattice parameters and mismatches in sulfur spacing for the djurleite Cu_{1.94}S-wurtzite ZnS system in possible interfacial directions

Lattice parameters	Cu _{1.94} S, <i>djurleite</i>	ZnS, <i>wurtzite</i>	Lattice mismatch, %
<i>a</i> (Å)	3.877	3.811	~1.70
<i>c</i> (Å)	6.716	6.234	~7.17
Angled (Å)	10.193	9.847	~3.39
<i>c/a</i> ratio	1.732	~1.636	/

- **Supplementary Materials: Table S3.**

Table S3. Peak identifications of XPS from survey spectra*

Samples	BE (eV)	Elements	Attributions	Spectral Lines
Cu _{1.94} S NCs	75.19	Cu	Cu _{1.94} S	<i>3p</i>
Cu _{1.94} S NCs	122.19	Cu	Cu _{1.94} S	<i>3s</i>
Cu _{1.94} S NCs	162.19	S	Cu _{1.94} S	<i>2p</i>
Cu _{1.94} S NCs	225.19	S	Cu _{1.94} S	<i>2s</i>
Cu _{1.94} S NCs	285.19	C	Organics	<i>1s</i>
Cu _{1.94} S NCs	549.19	Cu	Cu _{1.94} S	<i>Auger</i>
Cu _{1.94} S NCs	569.19	Cu	Cu _{1.94} S	<i>Auger</i>
Cu _{1.94} S NCs	648.19	Cu	Cu _{1.94} S	<i>Auger</i>
Cu _{1.94} S NCs	932.19	Cu	Cu _{1.94} S	<i>2p_{3/2}</i>
Cu _{1.94} S NCs	951.19	Cu	Cu _{1.94} S	<i>2p_{1/2}</i>
Cu _{1.94} S-ZnS NHs	10.19	Zn	ZnS	<i>3d</i>
Cu _{1.94} S-ZnS NHs	75.19	Cu	Cu _{1.94} S	<i>3p</i>
Cu _{1.94} S-ZnS NHs	89.19	Zn	ZnS	<i>3p</i>
Cu _{1.94} S-ZnS NHs	122.19	Cu	Cu _{1.94} S	<i>3s</i>
Cu _{1.94} S-ZnS NHs	139.19	Zn	ZnS	<i>3s</i>
Cu _{1.94} S-ZnS NHs	162.19	S	Cu _{1.94} S/ZnS	<i>2p</i>
Cu _{1.94} S-ZnS NHs	226.19	S	Cu _{1.94} S/ZnS	<i>2s</i>
Cu _{1.94} S-ZnS NHs	285.19	C	Organics	<i>1s</i>
Cu _{1.94} S-ZnS NHs	472.19	Zn	ZnS	<i>Auger</i>
Cu _{1.94} S-ZnS NHs	495.19	Zn	ZnS	<i>Auger</i>
Cu _{1.94} S-ZnS NHs	531.19	O	Environment	<i>1s</i>
Cu _{1.94} S-ZnS NHs	570.19	Cu	Cu _{1.94} S	<i>Auger</i>
Cu _{1.94} S-ZnS NHs	932.19	Cu	Cu _{1.94} S	<i>2p_{3/2}</i>
Cu _{1.94} S-ZnS NHs	951.19	Cu	Cu _{1.94} S	<i>2p_{1/2}</i>
Cu _{1.94} S-ZnS NHs	1021.19	Zn	ZnS	<i>2p_{3/2}</i>
Cu _{1.94} S-ZnS NHs	1044.19	Zn	ZnS	<i>2p_{1/2}</i>

* The BE peaks in survey spectra are directly read from the original data and may be slightly different from the corresponding BE peaks in high-resolution spectra. This is caused by the scanning accuracy induced deviation. The scanning increment for survey spectra was 1.0 eV/point, and the increment for high-resolution spectra was 0.05 eV/point.

References

- (1) Evans, H. T. The crystal structures of low chalcocite and djurleite. *Zeitschrift fur Kristallographie* **1979**, *150*, 299-320.
- (2) Wyckoff, R. W. G. Wurtzite structure. *Crystal Structures*, Second edition **1963**, *1*, 85-237.
- (3) Mumme, W. G.; Gable, R. W.; Petricek, V. The crystal structure of roxbyite, Cu₅₈S₃₂. *The Canadian Mineralogist* **2012**, *50*, 423-430.
- (4) Yamamoto, K.; Kashida, S. X-ray study of the average structures of Cu₂Se and Cu_{1.8}S in the room temperature and the high temperature phases. *Journal of Solid State Chemistry* **1991**, *93*, 202-211.